49th IEEE Conference on Decision and Control
December 15-17, 2010
Hilton Atlanta Hotel, Atlanta, GA, USA

Propulsive Energy Harvesting by a Fishlike Vehicle in a Vortex Flow: Computational Modeling and Control

Scott David Kelly and Parthesh Pujari

Abstract— **Using a model rooted in Hamiltonian mechanics, we consider the self-propulsion of a deformable planar hydrofoil in an ideal fluid in the presence of ambient vorticity, and investigate the mechanism whereby the hydrofoil can harvest energy from the surrounding flow in order to improve its own energy efficiency. We demonstrate, in particular, that energy harvesting can be achieved via closed-loop control without explicitly incorporating an assessment of the fluid velocity field into the feedback signal.**

I. INTRODUCTION

When marine animals or aquatic vehicles propel themselves in close proximity to one another, they interact hydrodynamically. Whether or not fish swim in schools to exploit such interactions for energetic advantage is a matter of persistent debate — early point and counterpoint are documented in [1] and [2] respectively — but it's straightforward to show experimentally [3] or computationally [4] that energetic advantage can be gained or lost according to the manner in which one body swims behind or beside another.

In the context of robotic locomotion — for the present paper, the swimming of a fishlike vehicle akin to many described in a literature initiated more than a decade ago [5] — this suggests a clear control problem: to determine the swimming strategy for given vehicle best suited to the harvesting of propulsive energy from a given surrounding flow. A persistent obstacle to the treatment of such problems via model-based control design is the paucity of mathematical models that capture the physics underpinning vortex-body interactions thoroughly enough to reproduce diverse flow conditions yet concisely enough to admit control-theoretic analysis. Models for aquatic locomotion in irrotational flows admit elegant analysis and treatment as control problems [6], [7], [8] but fail to address a central mechanism responsible for thrust development by real swimmers — to wit, vortex shedding — while high-fidelity computational models provide few points of entry for control engineers.

The authors and collaborators have recently developed an approach to modeling aquatic self-propulsion via vortex shedding in a manner that reproduces physically realistic planar fishlike swimming using principles from analytical mechanics, retaining a link to the formalism used in nonlinear control methods like energy shaping [9], which promise direct relevance to the issue of energy-efficient locomotion.

In the present paper, we do not approach an analytical solution to the control problem described above, but we use our model to investigate properties of efficient locomotion and empirical solutions to the energy-harvesting problem confronting a simple fishlike swimmer. In so doing we reveal, among other things, that the practical use of feedback control to achieve energy harvesting may not require the use of sensors to estimate the surrounding flow field, as is frequently supposed.

II. MODELING

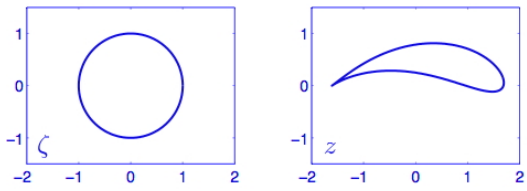

Fig. 1. Realization of an undulating fishlike contour as the image of a circle in the complex plane under a time-varying conformal transformation.

It was demonstrated in [10], following a line of research initiated with one of the authors in [11], that the planar mechanical system comprising a free rigid body of arbitrary shape interacting with a collection of point vortices in a perfect fluid admits a Hamiltonian structure. This structure persists when the body is allowed to deform over time; the amendment of the resulting system to allow discrete vortex shedding from the body in accordance with a time-periodic Kutta condition provides a simplified model for macroscopic swimming in water without explicitly addressing the role played by viscosity in boundary-layer formation and detachment. Such a model is detailed in [12] and summarized in [13]. We describe only certain relevant aspects of this model in the present paper, referring the reader to the aforementioned sources, but explore for the first time the diversity of propulsive mechanisms that it encapsulates.

We consider a swimming hydrofoil with only a single degree of freedom, its shape defined in the complex z plane as the image of a circle with radius r_c in the complex ζ plane under a time-varying Joukowski transformation of the form

$$z = F(\zeta) = \zeta + \zeta_c + \frac{a^2}{\zeta + \zeta_c}.$$

Support for this work was provided in part by NSF grants CMMI 04-49319 and ECCS 05-01407.

Scott David Kelly is with the Department of Mechanical Engineering and Engineering Science, University of North Carolina at Charlotte, Charlotte, NC 28223, USA scott@kellyfish.net

Parthesh Pujari is with the Department of Mechanical Engineering and Engineering Science, University of North Carolina at Charlotte, Charlotte, NC 28223, USA ppujari@uncc.edu

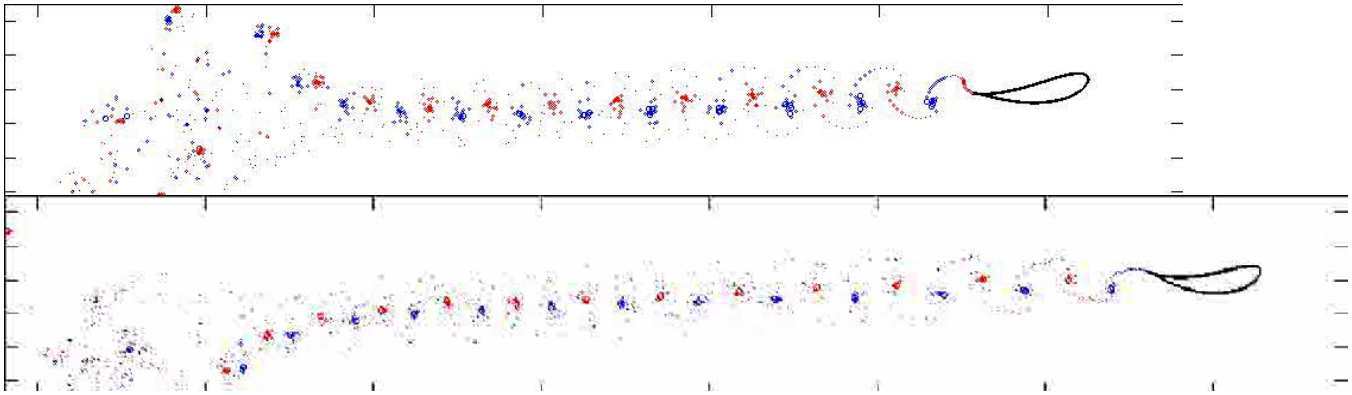

Fig. 2. Differences in propulsive efficacy and wake structure between sinusoidal (top) and piecewise linear (bottom) oscillations in camber. In these snapshots and in those that follow, red circles represent vortices with clockwise orientation and blue circles represent vortices with counterclockwise orientation. The size of each circle is proportional to the strength of the vortex it represents. Vortex strengths remain constant over time.

The parameters r_c, ζ_c, and a are assigned values according to a single time-varying shape parameter $s(t)$ that varies the camber of the foil while preserving its area. A representative deviation of the foil from zero camber, with $r_c = 1$, is depicted in Fig. 1.

If such a foil is surrounded by a collection of n point vortices, the strength of the kth vortex given by γ_k and its position given by $z_k = F(\zeta_k)$, then the coupled equations governing the motion of the foil and of the vortices are Hamiltonian with respect to a function

$$H = \frac{1}{2}\xi^T I \xi - 2\pi H_1,$$

where the terms in $\xi = [U\, V\, \Omega]^T$ correspond to the linear and angular velocity of the foil in a foil-fixed frame, I is the foil's shape-dependent effective inertia matrix, and

$$\begin{aligned} H_1 = &\sum_k \gamma_k \dot{s}\, \psi_s(x_k, y_k) \\ &- \frac{1}{2}\sum_k \gamma_k^2 \left(\log\left|\zeta_k\overline{\zeta_k} - r_c^2\right| + \log|F'(\zeta_k)|\right) \\ &+ \frac{1}{2}\sum_k \sum_{j\neq k} \gamma_k\gamma_j \left(\log|\zeta_k - \zeta_j| - \log\left|\zeta_k\overline{\zeta_j} - r_c^2\right|\right) \end{aligned}$$

is defined in terms of the stream function ψ_s determined by the shape of the foil.

In studying systems of point vortices in an ideal fluid, one must confront the fact that each vortex nominally induces an infinite rotational velocity at its own location, contributing an infinite *self-energy* to the system's total kinetic energy. The energy-like quantity that determines the Hamiltonian in the classical n-vortex problem is the *interaction energy* that remains when self-energy terms are removed from the formal kinetic energy [14]. What we refer to as the kinetic energy of the fluid in our system similarly omits vortex self-energy terms. One consequence of this convention is that what we call the fluid kinetic energy due to the influence of the vortices — a quantity that depends on logarithms of the distances between vortices, and is therefore measured relative to an arbitrary datum — may attain values less than zero. This doesn't alter the energy-like role played by this quantity, but can make plots of fluid energy versus time appear incorrect to the uninitiated.

The kinetic energy of the fluid in our problem admits the decomposition

$$KE = KE_b + KE_v, \tag{1}$$

where

$$KE_b = \frac{1}{2}\begin{bmatrix}\xi^T & \dot{s}\end{bmatrix}\begin{bmatrix} I & B \\ B^T & C\end{bmatrix}\begin{bmatrix}\xi \\ \dot{s}\end{bmatrix}$$

is the energy due to the motion of the body and

$$\begin{aligned} KE_v = &-\sum_k\sum_{j\neq k}\pi\gamma_k\gamma_j\log|\zeta_k - \zeta_j| \\ &+\sum_k\sum_j \pi\gamma_k\gamma_j\log\left|\zeta_k - \zeta_j^*\right| \\ &+\pi\left(\sum_k\gamma_k\right)\left(\sum_k\gamma_k\log\frac{|\zeta_k|}{r_c}\right) \end{aligned}$$

is the energy due to the influence of the vortices. Here B and C represent the body's shape-dependent effective inertia and ζ_j^* denotes the location of the *image vortex* within the circle in the ζ plane corresponding to the vortex at ζ_j [15]. When the body coasts longitudinally with its camber held at zero, KE_b is proportional to the square of the body's speed, and provides a measure of the body's own kinetic energy.

The decomposition (1) is possible because the fluid velocity due to the motion of the body is L^2-orthogonal to the fluid velocity due to the vortices. We couple the motion of the body to the distribution of vorticity in the fluid by introducing a vortex-shedding mechanism as follows. At regular intervals in time, a *Kutta condition* is applied at the foil's trailing point, requiring the introduction of new vortices at small distances offshore to enforce stagnation at the pre-image of the trailing point in the ζ plane. Different methods for determining the strengths and initial positions of new vortices are surveyed in [12]; simulations for the present paper employ a method described in [16], [17]. Concurrent with the Kutta condition,

we impose the requirement that the shedding of each new vortex preserve the total momentum in the fluid-foil system — effectively applying an impulsive force to the body with each shedding event to parallel the force experienced from real boundary-layer separation.

III. ENERGY EFFICIENCY AND WAKE STRUCTURE

To preface our discussion of energy harvesting, we highlight certain aspects of the relationship between the physical structure of a distribution of vortices and the transport of energy and momentum within that distribution of vortices. Figure 2 depicts snapshots from two simulations of the foil described in Section II propelling itself from rest in an otherwise quiescent fluid. The upper panel depicts the position of the foil and the structure of its wake after twenty sinusoidal oscillations in camber; the lower panel depicts the position of the foil and the structure of its wake after twenty triangle-wave oscillations in camber. The period of oscillation is the same in both cases, as is the economy of motion defined by the integral

$$\int_0^T |\dot{s}(t)|^2 \, dt \tag{2}$$

taken over one period of oscillation.

The scale is also the same in both panels; it's apparent that the sinusoidal gait is less effective than the triangle-wave gait in propelling the foil forward. In both cases, the structure of the foil's wake adheres to a paradigm emphasized in [5] and elsewhere, comprising coherent vortex structures of alternating sign loosely describing an inverse Kármán vortex street. On a more detailed level, however, the two wakes are clearly different. The authors feel that the novel reframing of the problem of optimal swimming as a problem of optimal wake generation promises to be fruitful, and are presently engaged in research along these lines.

The interaction energy within a pair of vortices with strengths Γ and $-\Gamma$, separated by a distance d, is proportional to $\Gamma^2 \log d$. The magnitude of the fluid impulse embodied in such a pair, directed transverse to the segment joining them, is proportional to Γd [18]. The generation of an energy-efficient propulsive wake by an isolated vehicle amounts, abstractly speaking, to shedding vorticity in a manner that maximizes momentum transport by the fluid relative to the energy imparted to the fluid. When vorticity is modeled discretely, this translates into a problem of optimizing the structure of a collection of linearly superposed vortex pairs.

A similar heuristic applies to the problem of energy harvesting. Presented with an ambient distribution of vorticity, an energy-harvesting swimmer's objective can be viewed as the realization of a wake incorporating both new and pre-existing vorticity such that fluid momentum is increased opposite the direction of swimming with a minimum investment of new energy in the fluid — or, more to the point, with a *negative* investment of new energy in the fluid.

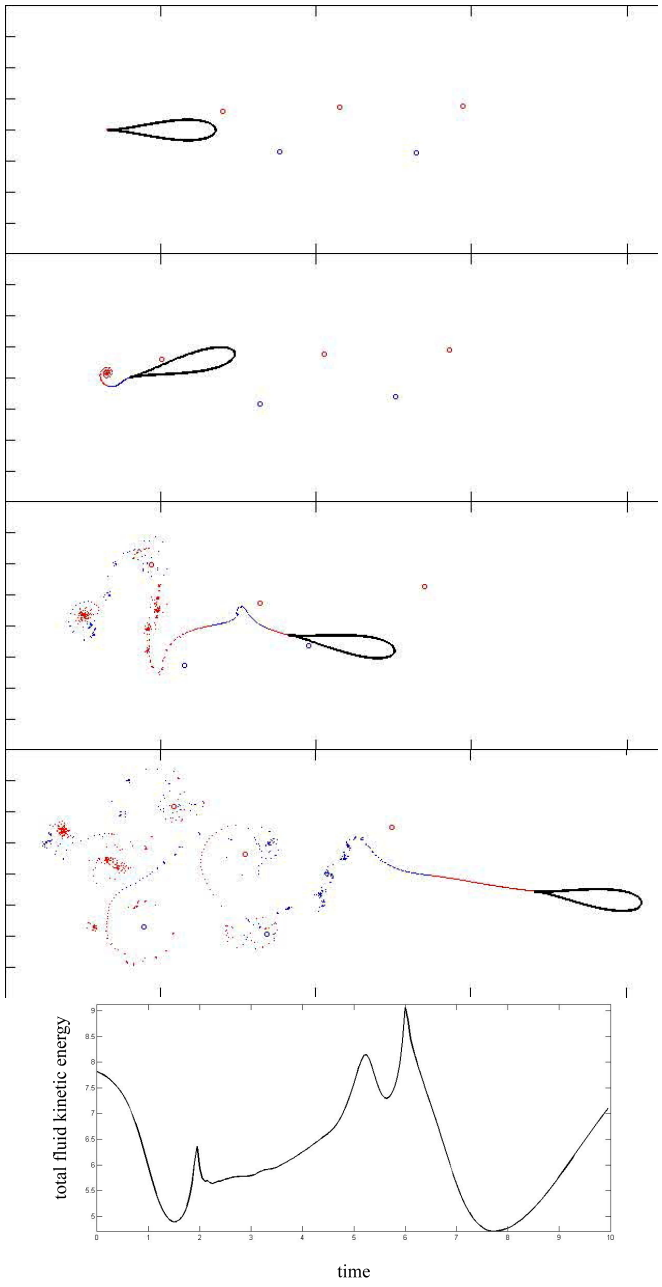

Fig. 3. Energy harvesting by a rigid foil, accelerated from rest by an ambient vortex street. The four frames shown are not equally spaced in time, but have been selected to illustrate different stages in the foil's motion.

IV. PASSIVE ENERGY HARVESTING

To illustrate the principle of energy harvesting in the simplest possible context, we present a simulation in which the camber of the foil is held fixed at zero and the foil is accelerated from rest by a judiciously constructed distribution of ambient vorticity evocative of the wake of a preceding vehicle. Four snapshots from this simulation appear in Fig. 3, accompanied by a plot of the total kinetic energy in the fluid versus time. The increase in the foil's kinetic energy is obvious from the foil's motion, and this motion contributes increasingly over time to the total kinetic energy of the fluid

through the KE_b term in (1), yet the total fluid energy initially decreases, reflecting a drop in the energy stored in vorticity. At the conclusion of the simulation, the foil is translating steadily away from the original vortices and the total fluid energy is approaching its original value from below.

V. STEERING VIA HEADING-ANGLE CONTROL

Before demonstrating that the foil can harvest energy through feedback control, we demonstrate that it can be steered successfully using a basic PID controller linking deviations in heading angle to the rate of change of the foil's camber, despite the significant nonlinearities present in the dynamics allowing the latter to influence the former.

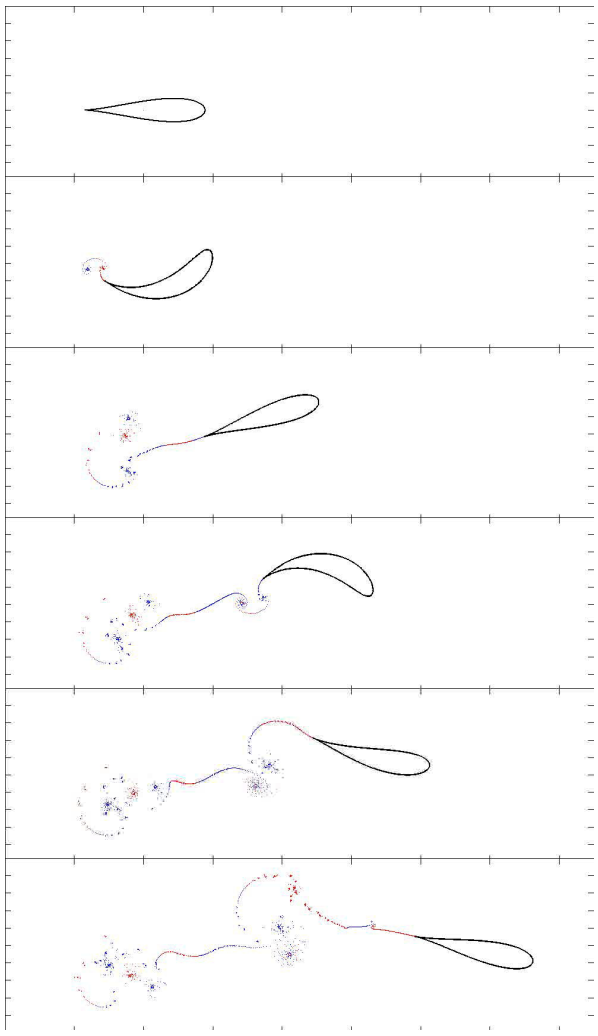

Fig. 4. A (3/10)-radian turn to the left followed by a (1/2)-radian turn to the right, initiated at rest, via PID control.

Figs. 4 and 5 depict the response of the controlled foil to step changes in its desired heading angle. In each case, the heading-angle error is input to an empirically tuned PID controller that specifies $\dot{s}(t)$ as its output. The dynamic similarity of the closed-loop system to a damped linear oscillator is particularly apparent in Fig. 5; the heading

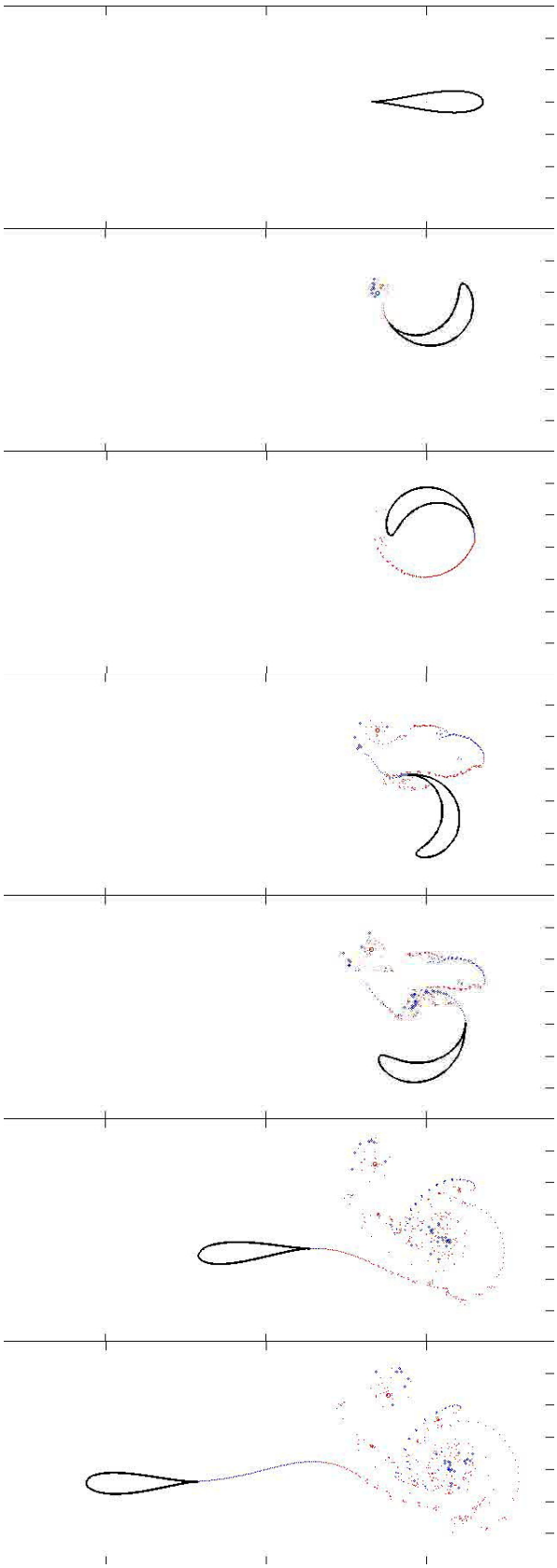

Fig. 5. A complete reversal in direction, initiated at rest, via PID control.

angle initially overshoots the desired value by more than two radians, then settles through one smaller oscillation to the desired value with no significant steady-state error. In both cases, a change in direction is necessarily followed by steady-state translation in the new direction.

VI. CONTROLLED ENERGY HARVESTING

Discussions of energy harvesting within fish schools frequently invoke the notion that fish use flow-sensing — more so, for instance, than vision [19] — in deciding how to tune their body motions for cooperative benefit. Artificial sensors patterned after the sensory organs of fish have been developed to assist in achieving the performance of swimming animals with robotic vehicles [20], but the practical imaging of the flow surrounding a robotic vehicle using only surface-mounted sensors presents significant technical challenges [21].

We present simulation data indicating that under at least certain circumstances, the implementation of heading angle control as described in Section V can allow our foil to harvest ambient vortex energy without explicit knowledge of the ambient flow field. Our preliminary interpretation of this phenomenon is as follows. When the foil encounters a distribution of vorticity that would otherwise cause it to veer one way or the other, a controller designed to stabilize the foil's heading angle will induce the foil to shed vorticity balancing that present in the fluid, in the sense that the resulting combined vorticity field will propel the foil in the desired direction. According to the heuristics of Section III, introducing vorticity of one sign in the proximity of vorticity with opposite sign will decrease the overall vortex energy present.[1]

Fig. 6 depicts the response of the controlled foil, initially at rest, to a step change in the desired heading angle. On the left at the top of the figure are the initial and final configurations of the system when no pre-existing vortex is present. On the right are the initial and final configurations of the system when a single clockwise vortex is initially present off the foil's port bow.

The overall control effort (not depicted) is slightly less in the presence of the pre-existing vortex, yet the final translational energy of the foil is greater, indicating greater speed. The fluid energy due to vorticity drops sharply as the initial deformation of the foil harvests energy from the pre-existing vortex, then rises as the translating foil sheds additional vortices.

The top panels in Fig. 7 place the foil in a situation similar to that depicted atop Fig. 3, confronted with a staggered array of vortices matching the orientation of the wake of another foil swimming upstream. The vortex array in Fig. 3, however, was constructed explicitly to engender passive energy harvesting by the rigid foil. The initial vortex array in Fig. 7 — laterally narrower than the array in Fig. 3 — is constructed to model one of the rolled-up wakes depicted in Fig. 2. The strengths of the individual initial vortices in Fig. 7 correspond, in particular, to the net strengths of the vortex patches in Fig. 2.

[1]In a viscous fluid, nearby vortices of opposite sign will actually annihilate each other. Vortex cancellation in fish locomotion is discussed in [22].

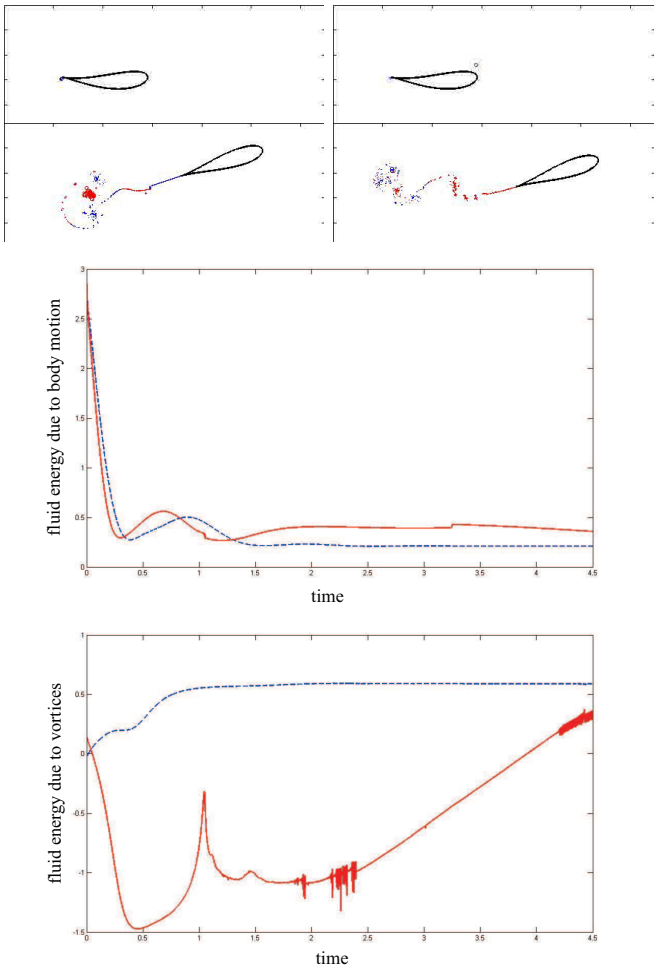

Fig. 6. Controlled energy harvesting from an isolated vortex. Solid red curves correspond to the case in which a vortex is present before the foil deforms (snapshots on the right), dashed blue curves to the case in which it is not.

On the left, we observe the behavior of the foil under heading-angle control. On the right, we observe the behavior of a rigid foil with the same initial conditions. As seen in Fig. 8, the final kinetic energy of the controlled foil is more than double that of the rigid foil, while the final vortex energy in the fluid is decreased with control — partly because the rigid foil is deflected to starboard by the vortex street.

One would expect, of course, that the use of control in this example — in essence, the exertion of swimming effort — would increase the final kinetic energy of the foil. It's therefore natural to ask whether or not open-loop swimming like that depicted in Fig. 2 would be a more effective use of control effort. Fig. 9 reproduces the final panel from the left of Fig. 7 alongside a snapshot of the final configuration of a foil that has applied the same total control effort to sinusoidal oscillatory swimming, failing to exploit the wake left behind by a predecessor swimming in this same fashion. The better strategy is clear.

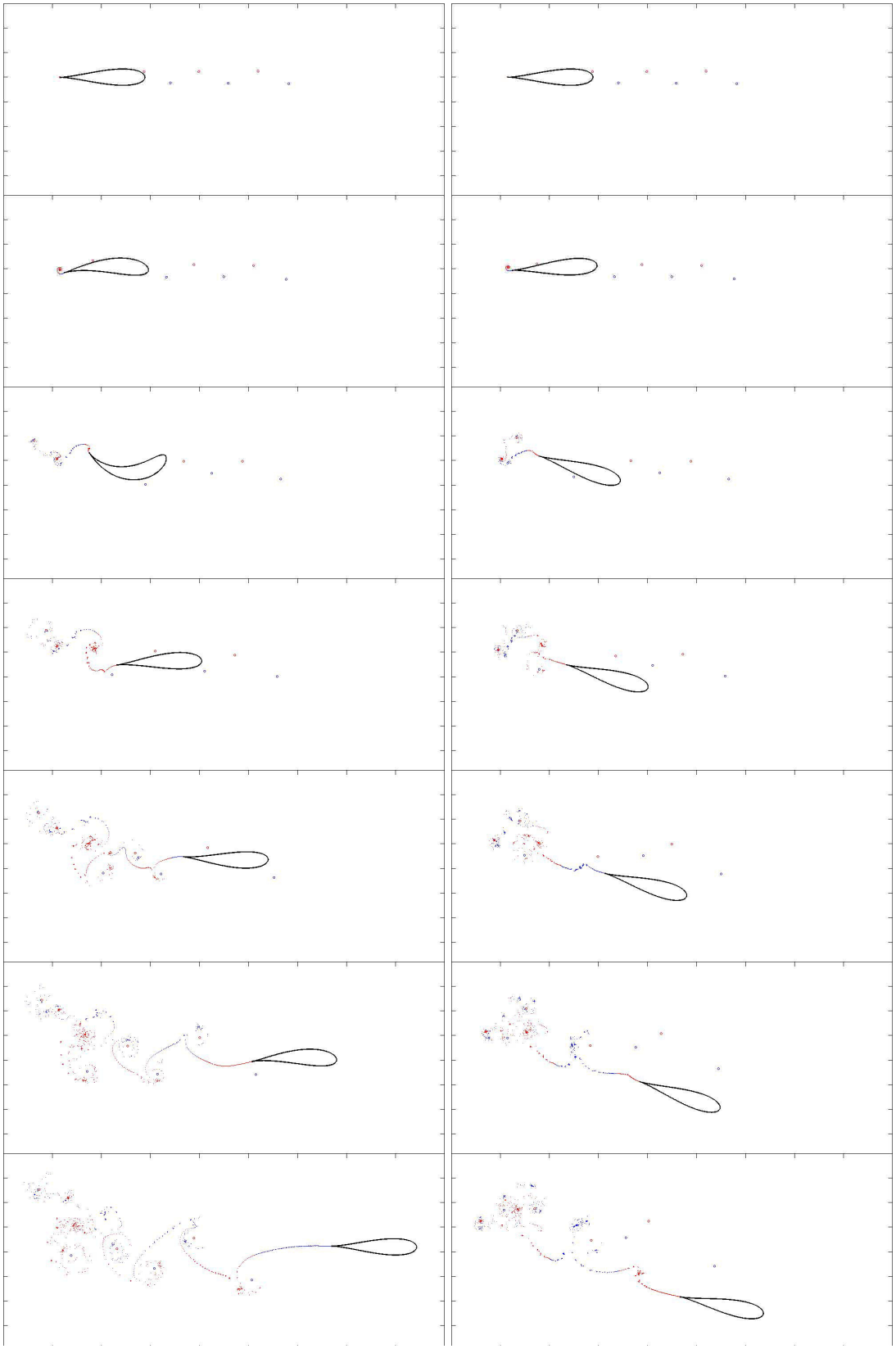

Fig. 7. Negotiating the wake of a preceding vehicle with (left) and without altering camber to stabilize heading angle. Stabilizing the foil's heading angle prevents its lateral ejection from the vortex street, and the corresponding changes in the foil's camber enhance the mixing of pre-existing vorticity with shed vorticity of opposite sign.

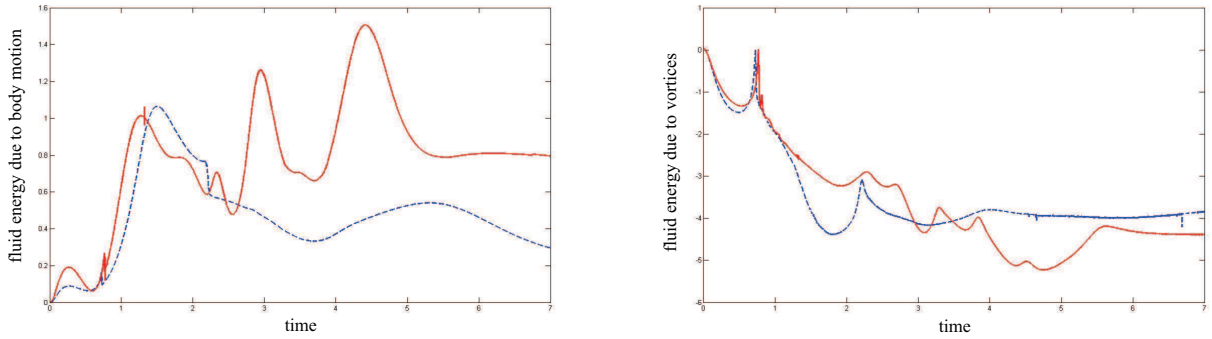

Fig. 8. The two components of fluid kinetic energy present in the simulations depicted in Fig. 7. Solid red curves correspond to the case in which the foil deforms, dashed blue curves to the case in which it does not.

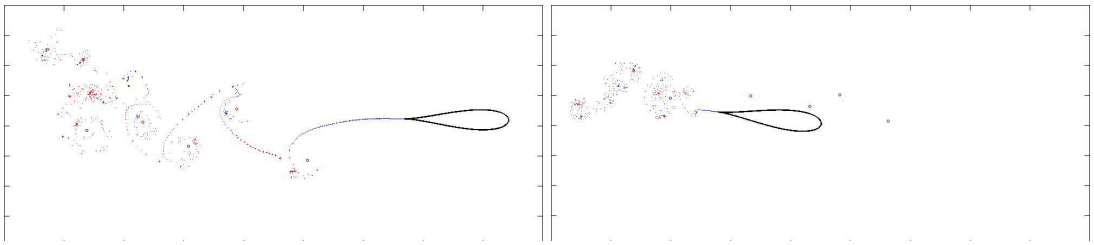

Fig. 9. Wake drafting using heading-angle control (left) versus oscillatory swimming as if no ambient vorticity were present. The economy of deformation, in the sense of (2), is the same in both cases; the displacement is greater in the former.

VII. FUTURE WORK

In addition to formalizing the control principles explored in the present paper and characterizing their limitations in an idealized setting, the authors intend to validate the predictions of their simulations experimentally in the immediate future. Members of the authors' research group have already developed a robotic platform capable of untethered locomotion in a manner morphologically similar to that of the foil modeled herein; experiments to date have focused on validating the relative merits of contrasting swimming gaits like those juxtaposed in Fig. 2.

REFERENCES

[1] V. V. Belyayev and G. V. Zuyev, "Hydrodynamic Hypothesis of School Formation in Fishes," *Problems of Ichthyology*, vol. 9, pp. 578–584, 1969.

[2] B. L. Partridge and T. J. Pitcher, "Evidence Against a Hydrodynamic Function of Fish Schools," *Nature*, vol. 279, pp. 418–419, 1979.

[3] S. D. Kelly and H. Xiong, "Controlled Hydrodynamic Interactions in Schooling Aquatic Locomotion," in *Proceedings of the 44th IEEE Conference on Decision and Control*, 2005, pp. 3904–3910.

[4] L. J. Zhang and J. Eldredge, "Hydrodynamics of Undulatory Fish Schooling in Lateral Configurations," 2010, arXiv:1003.4441v1 [physics.flu-dyn].

[5] M. S. Triantafyllou and G. S. Triantafyllou, "An Efficient Swimming Machine," *Scientific American*, vol. 272, pp. 64–70, 1995.

[6] S. D. Kelly, "The Mechanics and Control of Robotic Locomotion with Applications to Aquatic Vehicles," Ph.D. dissertation, California Institute of Technology, 1998.

[7] J. E. Radford, "Symmetry, Reduction and Swimming in a Perfect Fluid," Ph.D. dissertation, California Institute of Technology, 2003.

[8] E. Kanso, J. E. Marsden, C. W. Rowley, and J. B. Melli-Huber, "Locomotion of Articulated Bodies in a Perfect Fluid," *Journal of Nonlinear Science*, vol. 15, pp. 255–289, 2005.

[9] A. M. Bloch, D. Chang, N. E. Leonard, and J. E. Marsden, "Controlled Lagrangians and the Stabilization of Mechanical Systems II: Potential Shaping," *IEEE Transactions on Automatic Control*, vol. 46, no. 10, pp. 1556–1571, 2001.

[10] B. N. Shashikanth, "Poisson Brackets for the Dynamically Interacting System of A 2D Rigid Cylinder and N Point Vortices: the Case of Arbitrary Smooth Cylinder Shapes," *Regular and Chaotic Dynamics*, vol. 10, no. 1, pp. 1–14, 2005.

[11] B. N. Shashikanth, J. E. Marsden, J. W. Burdick, and S. D. Kelly, "The Hamiltonian Structure of a 2-D Rigid Circular Cylinder Interacting Dynamically with N Point Vortices," *Physics of Fluids*, vol. 14, pp. 1214–1227, 2002.

[12] H. Xiong, "Geometric Mechanics, Ideal Hydrodynamics, and the Locomotion of Planar Shape-Changing Aquatic Vehicles," Ph.D. dissertation, University of Illinois at Urbana-Champaign, 2007.

[13] S. D. Kelly and H. Xiong, "Self-Propulsion of a Free Hydrofoil with Localized Discrete Vortex Shedding: Analytical Modeling and Simulation," *Theoretical and Computational Fluid Dynamics*, vol. 24, no. 1, pp. 45–50, 2010.

[14] P. K. Newton, *The N-Vortex Problem*. Springer-Verlag, 2001.

[15] L. M. Milne-Thomson, *Theoretical Hydrodynamics*. Dover, 1996.

[16] K. Streitlien and M. S. Triantafyllou, "Force and Moment on a Joukowski Profile in the Presence of Point Vortices," *AIAA Journal*, vol. 33, no. 4, pp. 603–610, 1995.

[17] R. J. Mason, "Fluid Locomotion and Trajectory Planning for Shape-Changing Robots," Ph.D. dissertation, California Institute of Technology, 2002.

[18] S. H. Lamb, *Hydrodynamics*. Dover, 1945.

[19] T. J. Pitcher, B. L. Partridge, and C. S. Wardle, "Blind Fish Can School," *Science*, vol. 194, p. 964, 1976.

[20] Z. Fan, J. Chen, J. Zou, D. Bullen, C. Liu, and F. Delcomyn, "Design and Fabrication of Artificial Lateral Line Flow Sensors," *Journal of Micromechanics and Microengineering*, vol. 12, pp. 655–661, 2002.

[21] P. Li and S. Saimek, "Modeling and Estimation of Hydrodynamic Potentials," in *Proceedings of the 38th IEEE Conference on Decision and Control*, 1999, pp. 3253–3258.

[22] B. Ahlborn, D. G. Harper, R. W. Blake, D. Ahlborn, and M. Cam, "Fish Without Footprints," *Journal of Theoretical Biology*, vol. 148, pp. 521–533, 1991.